From superlattices to superatoms

E. A. Andryushin and A. A. Bykov

P. N. Lebedev Physics Institute of the Academy of Sciences of the USSR

Usp. Fiz. Nauk **154**, 123–132 (January 1988)

The development of modern technology to produce semiconducting materials with superstructures is without a doubt based on physical advances. Yet conversely this technology has become one of the main sources of new research fields in semiconductor physics. One such new field is mesoscopic physics[1]—the physics of intermediate-sized semiconductor superstructures. The word "superstructure" refers to the fact that in addition to the periodic potential of the crystalline lattice there exists in the system an additional potential, which is usually periodic as well. The characteristic scale and period of the additional potential are much larger than the lattice constant, so this potential may be described by macroscopic parameters, such as the permittivity. At the same time the potential scale is small enough for the existence of quantum size effects. In semiconductors the quasiparticle effective masses are usually much smaller than the free electron mass, whereas the Coulomb interaction between the quasiparticles is weakened by the permittivity. Consequently, the characteristic interaction energies are much smaller than atomic energies and corresponding length scales reach $\sim 10^2$ Å—the scale at which semiconductor superstructures may be described as mesoscopic.

Until recently experimental limitations confined physicists to studying semiconductor superlattices with a one-dimensional additional potential. The concept of such a superlattice was originally formulated by L. V. Keldysh in 1962, when he suggested that the periodic crystalline potential be modulated by an intense ultrasound wave.[2] In 1970, L. Esaki and R. Tsu proposed[3] and subsequently realized a composite superlattice—a superstructure produced by thin alternating layers of different semiconductor materials. In 1978, R. Dingle, H. Störmer, A. Gossard, and W. Wiegmann succeeded in selectively doping the superlattice[4] by intentionally doping selected superlattice layers. In 1981, K. Ploog, A. Fischer, G. Döhler, and H. Kunzel were the first to create a doped superlattice[5] in which the additional potential was introduced to the superconductor matrix by one-dimensional periodic modulation of donor and acceptor distributions. To date so many papers have been published on the subject of superlattices that even a list of review articles only would amount to a sizeable bibliography. A detailed discussion of this topic may be found in Refs. 6–8.

The 1980s witnessed the first attempts to create a more complex additional potential in the superlattice. Petroff and co-workers[9] were the first to realize experimentally the so-called "thread-like quantum well structure"—a system of semiconducting GaAs threads of up to 200×200 Å in cross-section imbedded in a $Ga_{1-x}Al_xAs$ matrix. Carrier motion in such a system is quasi-one-dimensional. Other recent results in the field include the creation of a "surface superlattice" in the inversion layer at the Si–SiO_2 interface,[10] deposition of a $GaAs/GaAs_{1-x}P_x$ superlattice with controlled variation of composition x in the plane of the layers,[11] as well as the production of two-dimensional heterostructure islands with in-plane diameter of ~ 50 μm[12]—the so-called "quantum discs," and so forth.

The possibilities of creating thin structures with ever smaller elements and ever more complex geometries have prompted many designs of new electronic devices: devices of minute size, working at higher speeds, requiring less power. In his introduction to a collection of papers [Ref. 8] L. Esaki termed the groundswell of activity in this field "the rebirth of semiconductor physics."

The concept of a "superatom"—a quasiatomic semiconductor heterostructure, first suggested by H. Watanabe in 1986, may prove quite important for the evolving "submicron" electronics.[13] In this paper we wish to discuss this concept, indicate the usefulness of quantum-mechanical theorems for superatomic calculations, and touch on the possible practical applications of these structures.

The superatom can consist of a selectively donor doped spherical semiconducting nucleus surrounded by an undoped semiconductor matrix with a smaller band gap. Donor electrons then escape to the matrix and the nucleus acquires a positive charge determined by the number of donors Z. Depending on the density of donors in the nucleus, given a reasonable nucleus diameter $d \sim 100$ Å, the quantity Z may reach several tens and even come to exceed the atomic numbers of all known elements in the periodic table. The minimal diameter of the nucleus required for a mesoscopic description is ~ 30 Å.

The first concrete computation of a superatom with an $Al_{0.35}Ga_{0.65}As$ nucleus and a GaAs matrix was carried out in Ref. 14.

The superatom is described by the nonrelativistic Schrödinger equation

$$\Psi'' + \frac{2}{r}\Psi' + \frac{2m}{\hbar^2}\left[E - V(r) - \frac{l(l+1)}{r^2}\right]\Psi = 0, \qquad (1)$$

where Ψ is the radial part of the wavefunction, E is the energy of the system, l is the orbital quantum number, r is the distance from the center of the nucleus, h is Planck's con-

 0038-5670/88/010068-06$01.80

stant, and m is the mass of the particle. In the case of a superatom the appropriate m is the effective electron mass, which may be different in the nucleus and the matrix.

The effective potential V of the superatom in (1) is spherically symmetric and consists of the following terms:[14]

$$V(r) = V_0 \cdot \theta(r_0 - r) + V_n(r)$$

$$+ V_{\text{Hartree}}(r) + V_{xc}(r); \qquad (2)$$

where r_0 is the radius of the nucleus, V_0 is the positive conduction band discontinuity between the nucleus and the matrix,

$$\theta(x) = 0, \quad x < 0,$$
$$= 1, \quad x \geqslant 0,$$

and V_n is the potential of the ionized donors. The Hartree potential $V_{\text{Hartree}}(r)$ and the exchange correlation potential $V_{xc}(r)$ are calculated using the customary approximations of the interacting electron gas theory. The main difference between the resulting potential and the potential of a heavy atom[15] consists of the following: the diameter of the nucleus is comparable to the entire extent of the superatom and hence there is no singularity at the origin. Consequently energy levels with higher orbital numbers l, for which the wavefunction peaks further away from the nucleus, are favored over the s-states.

In Ref. 14 the calculation was carried out with parameters $r_0 = 120$ Å and $Z = 20$ and resulted in the following ordering of levels: 1s, 2p, 3d . . . , as opposed to the usual atomic ordering of 1s, 2s, 2p, 3s, 3p, . . . The potential $V(r)$ corresponding to these parameters is plotted in Fig. 1. Various level configurations can be obtained by varying the parameters r_0 and Z. For example, $r_0 = 120$ Å corresponds to the ground state of $1s^2 2p^6 3d^{10} 2s^2$ for $Z = 20$, whereas $r_0 = 170$ Å corresponds to the ground state of $1s^2 2p^6 3d^{10} 2f^2$ at that same Z. The superatomic radius, nominally established by the peak of the radial wavefunction $\Psi_{2s}(r)$ of the 2s state ($Z = 20$, $r_0 = 120$ Å) is ≈ 355 Å, about three times larger than the radius of the nucleus. This sample calculation indicates that the properties of the superatom can vary widely depending on the potential $V(r)$, so it is helpful to get a picture of how the form of $V(r)$ affects the state of the system.

Here we direct the reader's attention to the fact that an analogous quantum-mechanical problem was studied quite extensively in high energy physics and the results obtained there could prove helpful for our semiconductor physics problem.

The problem of establishing general rules for the energy ordering of quantum-mechanical levels in a spherically symmetric potential arose in the field of heavy quarkonium spectroscopy, quarkonium being a bound quark-antiquark state. There mass m in formula (1) is the reduced mass $m = m_1 m_2/(m_1 + m_2)$ of the quark and antiquark masses m_1 and m_2, and V is their binding potential. Naturally, the quark masses are many orders of magnitude heavier than semiconductor quasiparticle masses, the energy scales are correspondingly different. For instance, the masses of c-quarks that make up J/Ψ particles (bound states of an c-quark with an $\bar{c}$-antiquark) are about 1.8 GeV, the mass of b-quarks that

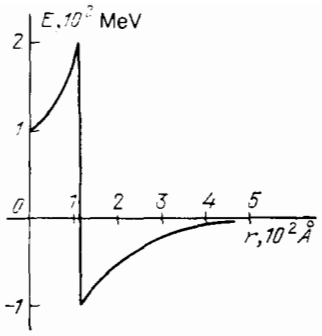

FIG. 1. Superlattice potential given by formula (2).

enter into γ-family particles is ≈ 5 GeV, and the mass of the hypothetical sixth t-quark is predicted to fall in the $m_t > 45$ GeV range. Accordingly the binding energies and characteristic length scales that determine the properties of such systems are of the order of $E \sim m\alpha_s^2 \sim 0.4$ GeV, $r \sim (m\alpha_s)^{-1} \sim 0.1$ fm at $\alpha \approx 0.2$ and $m \approx 50$ GeV. But the qualitative results cited below do not depend on these values.

A number of quantum-mechanical theorems on the ordering of $E(n, l)$ levels, where n is the principal quantum number and l is the orbital angular momentum of the system, have been proved in recent years.[16] The main criterion that determines the relative ordering of the levels is the curvature of the potential as compared to the Coulomb potential curvature

$$V_{\text{Coul}} \sim \frac{1}{r}. \qquad (3)$$

The following theorems have been rigorously proven:

I. *Depending on the sign of* $\Delta_r V$ *the following conditions are fulfilled*:

$$E(n, l-1) > E(n, l), \qquad (4)$$

if

$$Y_1 = \Delta_r V = \frac{d}{dr}\left(r^2 \frac{dV}{dr}\right) > 0, \qquad \forall r > 0,$$

and, conversely,

$$E(n, l-1) < E(n, l), \qquad (5)$$

if

$$Y_1 < 0, \quad \forall r > 0.$$

The case $Y_1 = 0$ corresponds to the Coulomb potential in which the energy levels are accidentally degenerate: $E(n, l-1) = E(n, l)$. Examples of potentials that correspond to conditions (4) and (5) are illustrated in Fig. 2.

II.

$$E(n, l) > E(n+1, l+2) \qquad (6)$$

if

$$Y_2 = \frac{d}{dr}\left(\frac{1}{r}\frac{dV}{dr}\right) > 0, \qquad \forall r > 0,$$

and, conversely,

$$E(n, l) < E(n+1, l+2) \qquad (7)$$

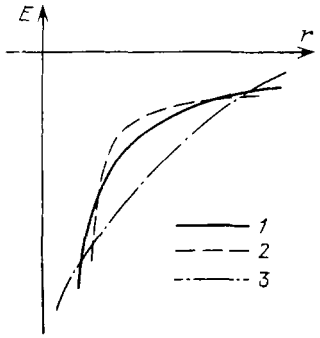

FIG. 2. Comparison of Coulomb potential (1), potential corresponding to condition (4) (2), and potential corresponding to the opposite condition (3)

if

$$Y_2 < 0, \ \forall r > 0.$$

The case $Y_2 = 0$ corresponds to the harmonic oscillator potential $V_{osc} \sim r^2$, in which case $E(n, l) = E(n+1, l+2)$.

In the perturbation theory approximation a number of other relations between neighboring levels have been established; in particular

III.

$$2E(n, l+1) \gtrless E(n-1, l) + E(n, l), \tag{8}$$

depending on the sign of

$$Y_2 \gtrless 0, \ \forall r > 0.$$

IV.

$$E(n+1, l) - E(n, l=0)$$

$$\gtrless E(n, l=0) - E(n-1, l=0) \tag{9}$$

depending on the sign of

$$Y_3 = \frac{d}{dr}\left[r^5 \frac{d}{dr}\left(\frac{1}{r}\frac{dV}{dr}\right)\right] \gtrless 0$$

for

$$\forall r > 0 \text{ and } u \lim_{r\to 0} r^3 V = 0.$$

There are grounds for believing theorem III to be valid without perturbation theory approximations. Theorem IV, on the other hand, loses its validity if the perturbations that disturb the monotonic character of potential V are large.

The above results apply only to potentials that have derivatives Y_i of definite sign. Potential (2) that is drawn in Fig. 1 exhibits a particular behavior which we describe by a θ-function or, simply, step function. In this case the quantities Y_i defined above change sign at the point $r = r_0$.

But the θ-functional potential was precisely the one proposed in the calculation of spectroscopic characteristics of heavy quarkonium with the aim of treating phase transitions that take into account the dynamical nature of quark mass.[17] The effect of the step function parameters on the energy levels and wavefunctions of the system can be evaluated either numerically or by perturbation theory methods.

The author of Ref. 18 used perturbation theory to calculate the effects of a model potential

$$V_1(r) = -\frac{B}{r} - V_0\theta(r_0 - r). \tag{10}$$

The potential V_1 is plotted in Fig. 3. It should be noted that the step in V_1 is opposite in sign from the step in the potential (2), but in the perturbation theory approximation all level shifts are proportional to V_0, which determines their sign. The opposite cases of (2) and (10) correspond to a potential "core" or "well" at the origin respectively.

The shift in the energy difference between 2s and 1s levels in the field of potential (10) is expressed by the formula

$$\Delta(E_{2s} - E_{1s}) = \frac{3}{8} + V_0 e^{-r_0}\left[1 + r_0 + \frac{r_0^2}{2} + \frac{r_0^4}{8} - e^{-r_0}(1 + 2r_0 + 2r_0^2)\right], \tag{11}$$

in Coulomb units with r_0 measured in units of Bohr radii $a_{Bohr} = \hbar^2/mB$. The shift (11) is always positive and peaks in the neighborhood of $r_0 \sim 2$. Consequently, in the field of potential (10) the θ-function always increases the energy difference between 2s and 1s levels, whereas in the superatomic potential (2) the energy difference is diminished.

The splitting of the 2s and 2p levels in potential (10) is more complicated and relevant to our problem:

$$\Delta(E_{2s} - E_{2p}) = \frac{V_0}{12} r_0^3 (r_0 - 2) e^{-r_0}. \tag{12}$$

At $r_0 = 2$ the Coulomb degeneracy $E_{2s} = E_{2p}$ persists. If $r_0 < 2$ the 2s level lies below the 2p level. But in the superatomic case V_0 is negative and at sufficiently small r_0 the 2p level lies lower.

At this point the reader might reasonably ask whether this derivation contradicts the results of Ref. 14 (discussed earlier in this review), wherein the f-states come to be favored over the s-states as the dimensions of the superatom increase. It so happens that the above analytic results apply to p-states, while the case of the f-states requires additional analysis. Furthermore, calculations taking V_0 as a perturbation parameter lose their validity in the case of f-states, when V_0 becomes comparable in magnitude to the total potential V.[1)]

In the field of a more complicated trial potential

$$V'(r) = -\frac{B}{r} + \frac{A}{r^2} - V_0\theta(r_0 - r) \tag{13}$$

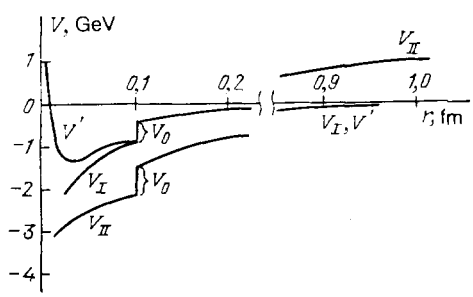

FIG. 3. Plots of potential V_1 (10), potential V' (13), and potential V_{II} used in calculating the properties of heavy quarkonium.

the energy splitting of the 2s and 2p levels is described by the expression[18]

$$E_{2s}-E_{2p}=\frac{AB^2m^2}{6\hbar^4}+\frac{V_0}{12}\Big[r_0^3(r_0-2)\,e^{-r_0}-32\,\frac{mA}{\hbar^2}E_1(-r_0)\cdot+\frac{4mA}{3\hbar^2}e^{-r_0}\left(r_0^5-\frac{34}{3}r_0^4+\frac{11}{3}r_0^3-18r_0^2-24r_0\right)+\frac{8mA}{3\hbar^2}e^{-r_0}(C+\ln r_0)\,(2r_0^4-r_0^3\cdot+6r_0^2+12r_0+12)\Big],\tag{14}$$

where C is Euler's constant, $E_i(x)$ is the exponential integral.

The second term of the potential (13) represents a repulsive core at the origin. It introduces into the splitting (14) a constant positive term $AB^2m^2/6\hbar^4$, as well as shifting the zero of (14) towards higher values of $r_0 > 2$. Expression (14) is qualitatively similar to (12) and reduces to the latter expression if $A = 0$. Consequently, in the case of the potential (13), a repulsive core also makes the 2p level relatively more favorable.

In addition, we have carried out numerical calculations for the V_{II} potential, which is sketched in Fig. 3. This potential is much more realistic in the quarkonium problem than the model potentials V_I and V' that could be handled by perturbation theory. This potential is characterized by the following behavior: $V_{II}(r) \sim r^{-1}\ln(\Lambda r)$ as $r \to 0$ and $V_{II}(r) \sim ar$ as $r \to \infty$, where $\Lambda = 0.1$ GeV and $a \approx 0.2$ GeV^2 are dimensional parameters. At the matching point r_0 of the two asymptotic expressions there is a θ-function singularity which corresponds to a transition from a phase with chiral symmetry to a phase without such symmetry.

The 2s-1s level splitting in this potential is determined mainly by the location and height of the step (the system is "confined" to a narrow and deep potential well. The $ns-(n-1)s$ level splitting is determined by the well width, whereas the depth fixes the number of approximately equidistant levels in the well). The 2s-1s level splitting exhibits the following asymptotic behavior. As $r_0 \to 0$, regardless of the step height V_0, the splitting tends towards typical values for a smooth quarkonium potential: $E_{2s}-E_{1s} \approx 700$:800 MeV at $m_q \approx 45$ GeV.[20] At higher r_0 the rate at which the $r_0 \to \infty$ asymptotic behavior is approached depends strongly on the step height. At $V_0 = 0$ the part of the potential that determines the property of low-lying bound states is dominated by the "soft" term (proportional to $r^{-1}\ln(\Lambda r)$) in the interactional potential—therefore $E_{2s}-E_{1s}$ tends towards values appropriate for this term, $E_{2s}-E_{1s} \approx 550$ MeV. At $V_0 = 600$ MeV this asymptotic behavior is reached much later, because the 2s-state, which has a mean-square radius $\langle r^2\rangle_{2s}^{1/2} \approx 0.17$ fm at $m_q = 45$ GeV, is "squeezed out" towards higher E_{2s} values by the step.

The 2s-2p level splitting is more complicated in the V_{II} potential. just as in the 2s-1s case, the energy level splitting decreases with step height V_0. The dependence of the splitting on the θ-function character of the potential is no longer monotonic, however. In the $r_0 \to 0$ limit (smooth potential) we obtain splittings similar to those produced in spectroscopy by standard quarkonium potentials: $\Delta(E_{2s}-E_{2p}) = 800$ MeV at $m_q = 45$ GeV. (This limit is not yet reached by thecurves plotted in Fig. 4.) As for the $r_0 \to \infty$ limit, the 2s-2p level splitting, like the 2s-1s splitting, tends towards values characteristic of the $V \sim r^{-1}\ln(\Lambda r)$ potential, $E_{2s}-E_{2p} \approx 130$ MeV—in this limit the mean-square radii of bound states are $\langle r^2\rangle 1/2 < r_0$ and the "soft" potential asymptotic behavior dominates. For the same reasons as in the 2s-1s case, the rate at which asymptotic values of $E_{2s}-E_{2p}$ are approached depends strongly on the height V_0 of the θ-function term: the asymptotic behavior is approached markedly slower at $V_0 = 600$ MeV than at $V_0 = 0$. The values of $\Delta(E_{2s}-E_{2p})$ at intermediate r_0 have a sign-changing functional dependence, which is plotted in Fig. 4.

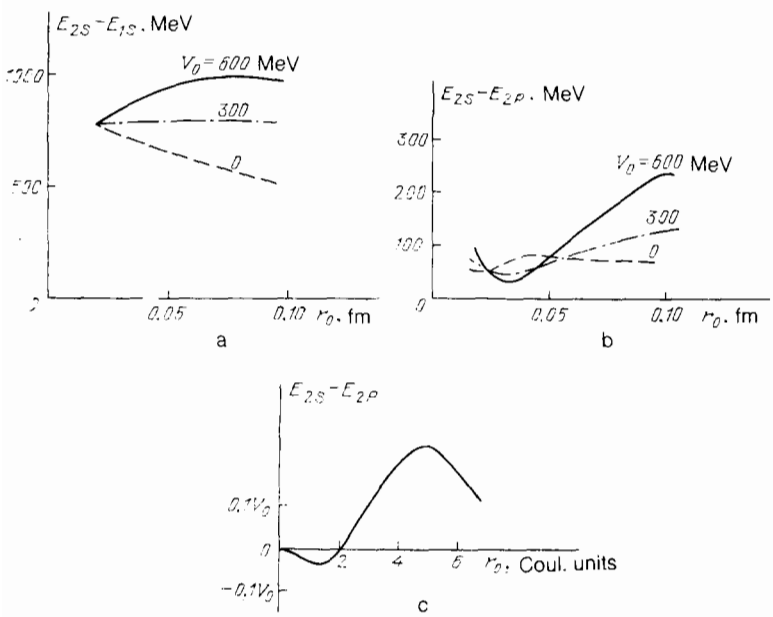

FIG. 4. Energy level splittings $E_{2s}-E_{1s}$ (a) and $E_{2s}-E_{2p}$ (b) in potential V_{II}, and $E_{2s}-E_{2p}$ (c) in potential (10).

Clearly the quantitative disagreement between the results plotted in these figures is due to the analytic model potentials and perturbation theory techniques—invalid in many regions—used in their derivation.

The behavior of the system wavefunction at the origin is also of interest. From the virial theorem of quantum mechanics, which states that the mean value of the kinetic energy depends on the potential gradient in the following manner:

$$\langle T\rangle = \frac{1}{2}\left\langle r\frac{dV}{dr}\right\rangle, \tag{15}$$

we obtain

$$|\Psi(0)|^2 \sim \left\langle m\frac{dV}{dr}\right\rangle. \tag{16}$$

Consequently, the θ-function singularity in the potential increases $|\Psi(0)|^2$ by

$$\Delta|\Psi(0)|^2 = m\,|\Psi(r_0)|^2 r_0^3 V_0. \tag{17}$$

The presence of the θ-functional singularity can markedly alter (from the case of a smooth potential) the relation

$$\frac{|\Psi(0)|^2_{n,l}}{|\Psi(0)|^2_{n+1,l}} \sim \frac{\langle dV/dr\rangle_{n,l}}{\langle dV/dr\rangle_{n+1,l}},$$

especially at small n and large quark masses. This happens, obviously enough, because at small n a fraction of the levels lies inside the step (mean-square radius of these states is smaller than r_0), while other levels lie outside (their mean-square radius is larger than r_0). Calculations show that, given $m_q \approx 45$ GeV, $|\Psi(0)|^2_{2s}/|\Psi(0)|^2_{1s} \approx 0.5$–$0.6$—twice the "standard" ratio $|\Psi(0)|^2_{2s}/|\Psi(0)|^2_{1s} \approx 0.25$-$0.3$ obtained from smooth potentials.

The numerically calculated results of $|\Psi(0)|^2$ behavior in the field of potential V_{II} as a function of position r_0 and magnitude V_0 of the θ-singularity are plotted in Fig. 5, whence it follows that the dependence of $|\Psi(0)|^2$ on parameters r_0 and V_0 is practically monotonic.

One final remark on the absolute values of the level energies in a step-containing potential as a function of particle mass. According to Feynman's theorem the following relation is valid

$$\frac{\partial E}{\partial m} \sim \left\langle r\frac{dV}{dr}\right\rangle.$$

The presence of a θ-singularity in the interaction potential increases the dependence of the energy of the system on particle mass (see potentials V_I, V_{II} of Fig. 3). In the case of superatomic potential (2) with a step of the opposite sign the energy becomes less dependent on mass. We expect quarkonium spectroscopy will succeed in measuring the relations

$$\frac{(\partial E/\partial m)_{2s}}{(\partial E/\partial m)_{1s}} \sim \frac{\langle r\,dV/dr\rangle_{2s}}{\langle r\,dV/dr\rangle_{1s}}$$

for the first two levels in the charmonium, bottomonium, and toponium families; like the ratio of $|\Psi(0)|^2_{2s}/|\Psi(0)|^2_{1s}$, these results will shed light on the position and magnitude of the θ-singularity in the potential.

Planned experiments on SLC and LEP e^+e^- accelerators, which will come on line between 1987 and 1990 probably will make possible a detailed investigation of the spectroscopic properties of toponium family particles. These data will clarify the behavior of the quark-antiquark interaction potential at distances < 0.1 fm and yield information on the dynamic behavior of quark mass. Measurement of 2s-1s and 2s-2p splittings with $\sim$ 100 MeV accuracy (bottomonium levels can be determined with accuracy of ~ 0.5 MeV), together with measurement of the $|\Psi(0)|^2_{2s}/|\Psi(0)|^2_{1s}$ ratio with ~ 0.10–0.15 accuracy (in bottomonium this ratio can currently be measured to 0.08 accuracy) will be sufficient for this task.

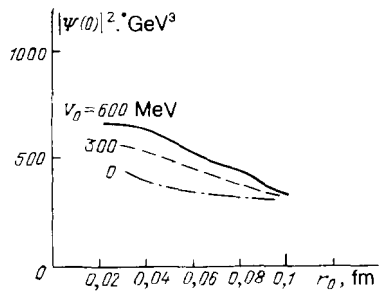

FIG. 5. Dependence of $|\Psi(0)|^2_{1s}$ on the position of the θ-function singularity in potential V_{II}.

The reason we have discussed the general theorems and their application to the quarkonium system in such detail is that they can prove quite helpful in understanding the properties of superatoms as well, once the appropriate scale changes are implemented.

Let us now return to the prospects of modelling systems with spherically symmetric potentials in solid state physics. Interestingly, the problem (1) has recently found yet another application. The authors of Ref. 21 experimentally measured the mass distribution of Na atom clusters. Among clusters of 4 to 100 Na atoms the main distribution maxima occured at $N = 2, 20, 40, 58$, and 92. This led to the observation that a cluster resembles a giant atom and the indicated numbers correspond to completely filled shells. This idea was confirmed by computation in Ref. 22, where equation (1) was solved using an average potential that takes into account electron screening of the cluster charge and electron-electron interaction. Generally speaking such clusters only nominally resemble atoms, since ions in a cluster are much less mobile than nucleons in a nucleus. Besides, the dimensions of a cluster with respect to the entire system are much larger. Still, in the case of alkali metals the ionic field is effectively screened by the valence electrons; after averaging the potential can be taken as spherically symmetric and the geometric structure of the cluster can be treated as a perturbation.[22]

The resulting potential differs from expression (2) by the absence of the first term—the discontinuous step—but the derivatives Y_i also change sign, and the calculated level ordering ls, 2s, 3d, 2s matches the superatom. Modern technological capabilities will likely permit the production of metallic clusters with yet more complicated types of potential $V(r)$.[23]

In all, if the superatom concept is actually realized it will become possible to construct systems with potentials that are quite varied and distinctive in their properties. Electrons in a superatom are bound to well-defined atomic orbitals and localized in the vicinity of the artificially construct-

ed nucleus. The superatomic ionization energy is ~ 1 MeV, so the states can be perturbed by relatively small fields. The creation of supermolecules, superatomic clusters and even supercrystals will probably become possible. Furthermore, the "supercrystalline lattice" can be created by design, choosing its period and symmetry. This opens up the possibility of studying the instability of the electronic subsystem when lattice recrystallization is impossible. This could make it possible to model and study physical effects that are difficult to realize in naturally occuring solids, for example the Wigner crystallization of a low density electron gas.

Properties of superatoms can be as varied as those of semiconducting materials.

The step height V_0 and quasiparticle mass can be varied over a wide range. It may also be possible to produce superantiatoms,[13] in which the nucleus is doped with acceptors and has a negative charge, with holes playing the role of bound quasiparticles. Interesting applications have been proposed for superatoms with all shells unfilled save the first and with the maximum orbital angular momentum. A single electron counter based on an ionized superatom has been proposed.[24] The possibility of constructing memory cells using superatomic structures was discussed in Ref. 13.

We hope that this article will draw further attention to the described physical phenomena.

[1)]One of the authors (E. A.) verified that in the perturbation theory approximation the ordering of s and f levels in the potential (10) agrees with that cited earlier in this paper.

[1]B. Schwarzschild, Phys. Today **39**(1), 17 (1986).
[2]L. V. Keldysh, Fiz. Tverd. Tela (Leningrad) **4**, 2265 (1962) [Sov. Phys. Solid State **4**, 1658 (1962)].
[3]L. Esaki and R. Tsu, IBM J. Res. Dev. **14**, 61 (1970).
[4]R. Dingle *et al.*, Appl. Phys. Lett. **33**, 665 (1978).
[5]K. Ploog *et al.* in: Gallium Arsenide and Related Compounds 1980, edited by W. H. Thim, Institute of Physics Conference Series No. 56, London, 1981.
[6]Two-Dimensional Systems, Heterostructures and Superlattices, edited by G. Baker, F. Kuchar, and H. Heinrich, Springer-Verlag, N.Y., 1984.
[7]A. P. Silin, Usp. Fiz. Nauk **147**, 485 (1985) [Sov. Phys. Uspekhi **28**, 972 (1985)].
[8]Heterojunctions and Semiconducting Superlattices; Proc. of the Winter School, Les Houches, France, March 12–21, 1985, edited by G. Allan, Springer-Verlag, N.Y., 1986.
[9]P. M. Petroff *et al.*, Appl. Phys. Lett. **41**, 635 (1982).
[10]A. C. Warren *et al.*, IEEE Electron. Device Lett. **6**, 294 (1985).
[11]S. M. Bedair, M. A. Tischler, and T. Katsuyama, Appl. Phys. Lett. **48**, 30 (1986).
[12]A. Scherer and H. G. Craighead, Appl. Phys. Lett. **49**, 1284 (1986).
[13]H. Watanabe and T. Inoshita, Optoelectron. Device Technol. **1**, 33 (1986).
[14]T. Ioshita, S. Ohnishi, and A. Oshiyama, Phys. Rev. Lett. **57**, 2560 (1986).
[15]See, for example: Methods of Electronic Structure Calculations for Atoms and Molecules (in Russian), edited by M. G. Veselov, Izd. Leningrad Univ., L., 1976.
[16]See, for example: A. Martin, CERN preprint CERN-TH. 4676/87, Geneva, 1987.
[17]A. A. Bykov and I. M. Dremin, Yad. Fiz. **44**, 1542 (1986) [Sov. J. Nucl. Phys. **44**, 1003 (1986)].
[18]L. I. Dremin, Kratk. Soobshch. Fiz. No. 1, 45 (1987) [Sov. Phys. Lebedev Inst. Rep. No. 1, 30 (1987)].
[19]See, for example: E. V. E. Kovacs, D. K. Sinclair, and J. B. Kogut Preprint ANL-HEP-PR-86-137 (1986).
[20]S. N. Gupta, S. F. Radford, W. W. Repko, Phys. Rev. Ser. D **34**, 201 (1986).
[21]W. D. Knight *et al.*, Phys. Rev. Lett. **52**, 2141 (1984).
[22]Y. Ishii, S. Ohnishi, and S. Sugano, Phys. Rev. B **33**, 5271 (1986).
[23]W. Ekardt, Phys. Rev. B **34**, 526 (1986).
[24]A. P. Silin, Fiz. Tverd. Tela **29** (Leningrad) (1987) [Sov. Phys. Solid State 29 (1987)].

Translated by A. Zaslavsky